International Journal of Biological Macromolecules 119 (2018) 1027–1035

Contents lists available at ScienceDirect

International Journal of Biological Macromolecules

journal homepage: http://www.elsevier.com/locate/ijbiomac

Structure and inflammatory activity of the LPS isolated from *Acetobacter pasteurianus* CIP103108

Mateusz Pallach [a], Flaviana Di Lorenzo [a], Fabio Alessandro Facchini [b], Djamel Gully [d], Eric Giraud [d], Francesco Peri [b], Katarzyna A. Duda [c,e], Antonio Molinaro [a], Alba Silipo [a,*]

[a] Department of Chemical Sciences, University of Napoli Federico II, Complesso Universitario Monte Sant'Angelo, Via Cintia 4, I-80126 Napoli, Italy
[b] Department of Biotechnology and Biosciences, University of Milano-Bicocca, Piazza della Scienza 2, 20126 Milano, Italy
[c] Junior Group of Allergobiochemistry, Research Center Borstel, Leibniz Lung Center, 23845 Borstel, Germany
[d] IRD, Laboratoire des Symbioses Tropicales et Méditerranéennes (LSTM), UMR IRD/SupAgro/INRA/UM2/CIRAD, TA-A82/J – Campus de Baillarguet, 34398 Montpellier Cedex 5, France
[e] Airway Research Center North (ARCN), German Center for Lung Research, Germany

ARTICLE INFO

Article history:
Received 16 May 2018
Received in revised form 6 August 2018
Accepted 7 August 2018
Available online 8 August 2018

Keywords:
Lipopolysaccharides (LPS)
Gram-negative bacteria
Innate immunity
MD2-TLR4
Acetobacter pasteurianus

ABSTRACT

Acetobacter pasteurianus is an acetic acid-producing Gram-negative bacterium commonly found associated with plants and plant products and widely used in the production of fermented foods, such as kefir and vinegar. Due to the acid conditions of the bacterium living habitat, uncommon structural features composing its cell envelope are expected. In the present work we have investigated the *A. pasteurianus* CIP103108 lipopolysaccharide (LPS) structure and immunoactivity. The structure of the lipid A and of two different *O*-polysaccharides was assessed. Furthermore, immunological studies with human cells showed a low immunostimulant activity of the isolated LPS, in addition to a slight capability to lower the NF-kB activation upon stimulation by toxic LPS.

1. Introduction

Gram-negative bacteria can be found in different habitats, many used within human activities as production and processing of traditional foods and beverages, in biotechnology and genetic engineering, in the production of pharmaceuticals [1]. A fascinating example is given by *Acetobacter pasteurianus*, an acetic acid-producing bacterium [2,3] commonly found associated with plants and plant products and present on sugar-rich substrates such as fruits, flowers and vegetables. *A. pasteurianus* is used in the production of fermented foods, such as kefir and vinegar [4] and, together with other microorganisms such as *Aspergillus oryzae*, *Saccharomyces cerevisiae* and lactic acid bacteria, is used in production process of Japanese black rice vinegar, called *kurozu* [5], whose consumption is believed to carry significant benefits to human health in cancer prevention and relief of hypertension [6].

A. pasteurianus, as most Gram-negative bacteria, possesses an outer membrane which predominantly contains lipopolysaccharides (LPS) on the outer leaflet [7]. The LPS is an amphiphilic molecule typically constituted by three different domains in the so called "smooth" form (S-LPS): the glycolipid anchoring the LPS to the outer membrane is called lipid A and is commonly made up of a variously acylated *bis*-phosphorylated glucosamine disaccharide backbone [8,9]. A core oligosaccharide (core OS) is attached to the lipid A through the 3-deoxy-D-*manno*-oct-2-ulosonic acid (Kdo), a sugar marker of Gram-negative bacteria. To the core OS is, in turn, connected a polysaccharide termed *O*-specific polysaccharide or *O*-chain [10]. Being the most exposed moiety of the LPS, the *O*-chain is in direct contact with the surrounding environment and is involved in interaction with host cells in case of pathogen and symbiont bacteria [11,12].

The LPS is classified as a microbe associated molecular pattern (MAMP) and it can activate the innate immune response following its recognition by immune receptors referred to as pattern recognition receptors (PRR) [8]. In mammals, LPS is recognized by the Toll-like Receptor 4/Myeloid differentiation factor-2 (TLR4/MD-2) receptor complex [13,14]. The center of LPS immunoactivity lies in the lipid A portion, specifically bound by the TLR4/MD-2 complex and differently activating the production of pro-inflammatory cytokines depending on its fine structure [8]. This event is beneficial to the host, enhancing resistance to infecting microbes, nonetheless excessive activation of TLR4/MD-2 signalling by agonistic LPS leads to massive and uncontrolled cytokines release finally leading to septic shock and multi-organ failure. Intriguingly, some lipid A showed a weak or no immunopotency and, in

* Corresponding author.
E-mail addresses: mateusz.pallach@unina.it (M. Pallach), flaviana.dilorenzo@unina.it (F. Di Lorenzo), f.facchini@campus.unimib.it (F.A. Facchini), djamel.gully@ird.fr (D. Gully), eric.giraud@ird.fr (E. Giraud), francesco.peri@unimib.it (F. Peri), kduda@fz-borstel.de (K.A. Duda), molinaro@unina.it (A. Molinaro), silipo@unina.it (A. Silipo).

https://doi.org/10.1016/j.ijbiomac.2018.08.035

some cases, an inhibition of the toxic effects of pathogenic LPS on TLR4/MD-2 expressing cells [15–21]. Given this premise, investigation on novel lipid A structures, which might possess inhibitory activity towards TLR4/MD-2 mediated release of pro-inflammatory cytokines by toxic lipid A, are considered of high relevance.

Here, we report the structural characterization of LPS *O*-antigen and lipid A from *A. pasteurianus* strain CIP 103108, performed by the combined use of chemical, NMR spectroscopy and mass spectrometry (MS) approaches. Furthermore, we also evaluated the immunostimulant activity of the isolated LPS on human cell lines showing interesting inhibitory effects against potent toxic LPS.

2. Experimental

2.1. Extraction and purification of A. pasteurianus CIP103108 LPS

Dried *A. pasteurianus* CIP103108 cells were washed with ethanol, water and acetone. Afterwards, the hot phenol/water procedure was employed to extract the LPS material [22]. After dialysis against distilled water, each phase, namely the water phase (WP) and phenol phase (PP) underwent enzymatic digestion using DNAse, RNAse and proteinase K. WP and PP were analyzed by 14% sodium deoxycholate-polyacrylamide gel electrophoresis (DOC-PAGE) analysis followed by silver nitrate gel staining. A size exclusion chromatography on a Sephacryl S200 column in denaturing conditions (0.25% DOC at pH 8) was performed to further purify the LPS material. Fractions were lyophilized and DOC was removed by ethanol washing, followed by extensive dialysis against distilled water. Each fraction was analyzed by sodium dodecyl sulfate-polyacrylamide gel electrophoresis (SDS-PAGE).

2.2. Monosaccharide compositional analysis of A. pasteurianus CIP103108 LPS

The neutral sugar constitution was established using acetylated alditols method [23]. An aliquot of sample was hydrolyzed using 2 M TFA solution at 120 °C for 120 min. The so obtained monosaccharides were reduced to alditols using $NaBH_4$ and then acetylated twice with equal amounts of acetic anhydride in pyridine at 85 °C for 10 min. The acetylated alditols were analyzed by gas-liquid chromatography/mass spectrometry (GLC-MS). For quantification 3 μg of xylose as internal standard was added to the sample. Amino sugars were characterized using 16 h hydrolysis in 4 M HCl at 100 °C, followed by reduction and acetylation as described above. The uronic acids composition was characterized using the same method as neutral sugars but preceded by additional reduction of the carboxyl group with $NaBD_4$. Ulosonic acids were identified using acetylated methyl glycosides method [23]. The sample underwent 16 h methanolysis with 1.25 M HCl/MeOH at 85 °C, therefore was acetylated as described above. Linkage analysis was performed using Ciucanu-Kerek's method [24]. An aliquot of LPS was suspended in DMSO and methylated with iodomethane in presence of NaOH. Therefore, the product was hydrolyzed with 2 M TFA for 2 h at 120 °C, reduced with $NaBD_4$ and acetylated with acetic anhydride in pyridine. Partially methylated acetylated alditols were analyzed by GC–MS.

2.3. Fatty acid compositional analysis of A. pasteurianus CIP103108 LPS

Total fatty acid content was characterized as fatty acid methyl esters. An aliquot of LPS was hydrolyzed using 4 M HCl at 100 °C for 4 h. After the sample was neutralized with 5 M NaOH for 30 min at 100 °C. Liberated fatty acids were extracted with chloroform and methylated using diazomethane at room temperature. In order to elucidate the position of hydroxyl group of hydroxy fatty acids 2 h derivatization with *N,O-bis*-(trimethylsilyl)trifluoroacetamide (BSTFA) at 65 °C was performed. Ester linked fatty acid content was characterized using 30 min hydrolysis with 0.5 M NaOH in water:methanol solution (1:1) at 100 °C for an hour. The ester linked fatty acids were extracted and methylated as described above. Fatty acid methyl esters were detected by GLC [HP 6890 N gas chromatograph with FID and a column (Agilent Technologies, 30 m × 0.25 mm, film thickness 0.25 μm) of Phenyl MethylSiloxane HP-5MS] with temperature program as follows: 120 °C for 3 min, then 5 °C min^{-1} to 320 °C.

2.4. Isolation of lipid A and O-polysaccharide moieties

To separate the lipid A and the polysaccharide portion constituting the *A. pasteurianus* CIP103108 LPS, a mild acid hydrolysis with acetate buffer (pH 4.4) for 5 h at 100 °C was performed. The glycolipid part was separated from the hydrophilic carbohydrate part using Blight-Dyer's method [25]. Briefly, a mixture of methanol and chloroform was added to the sample to reach a ratio of chloroform/methanol/hydrolysate 2:2:1.8 (v/v/v). The mixture was shaken and centrifuged. The water-soluble phase was then applied on a GE Healthcare Life Sciences Superdex 75 column eluted with 50 mM ammonium bicarbonate. The chromatography fractions were then monitored by NMR spectroscopy. The lipid A part was also collected, lyophilized and analyzed by MALDI MS.

2.5. MALDI-TOF MS and MS/MS

Reflectron MALDI-TOF MS and MS/MS analysis were performed on an ABSCIEX TOF/TOF™ 5800 Applied Biosystems mass spectrometer equipped with an Nd:YLF laser with a λ of 345 nm, a <500-ps pulse length and a repetition rate of up to 1000 Hz. The lipid A fraction was dissolved in $CHCl_3$/MeOH (1:1, v/v) as previously described [26,27]. The matrix was the trihydroxyacetophenone (THAP) dissolved in CH_3OH/0.1% TFA/CH_3CN (7:2:1, v/v/v) at a concentration of 75 mg ml^{-1}. Lipid A solution and the matrix solution, both 0.5 μl, were deposited on the MALDI plate and dried at room temperature. All of spectra were a result of the accumulation of 1500 laser shots, whereas 6000–7000 shots were summed for the MS/MS data acquisitions [28].

2.6. NMR spectroscopy

For structural assignments of isolated polysaccharides ^1H NMR and 2D NMR spectra were recorded in D_2O at 278 K at pD 7 with a cryoprobe-equipped Bruker 600 DRX spectrometer. Total correlation spectroscopy (TOCSY) experiments were performed with spinlock times of 100 ms using data sets (t1 × t2) of 4096 × 512 points. Rotating-frame Overhauser enhancement spectroscopy (ROESY) and nuclear Overhauser enhancement spectroscopy (NOESY) experiments were performed using data sets (t1 × t2) of 4096 × 512 points with mixing times between 100 and 400 ms. Double-quantum-filtered phase-sensitive correlation spectroscopy (DQF-COSY) experiments were performed using data sets of 4096 × 912 points. The data matrix in all homonuclear experiments was zero-filled in both dimensions to give a matrix of 4 K × 2 K points and was resolution-enhanced in both dimensions using a cosinebell function before Fourier transformation. Coupling constants were determined by 2D phase-sensitive DQF-COSY measurements [29,30]. Heteronuclear single-quantum coherence (HSQC) and heteronuclear multiple-bond correlation (HMBC) experiments were performed in the ^1H-detection mode by single-quantum coherence with proton decoupling in the ^{13}C domain using data sets of 2048 × 400 points. HSQC was performed using sensitivity improvement and in the phase-sensitive mode using echo/antiecho gradient selection, with multiplicity editing during the selection step [31]. HMBC was optimized on long-range coupling constants, with a low-pass *J* filter to suppress one-bond correlations, using gradient pulses for selection. Moreover, a 60 ms delay was used for the evolution of long-range correlations. HMBC spectra were optimized for 6–15 Hz coupling constants. The data matrix in all the heteronuclear experiments was extended to

2048 × 1024 points by using a forward linear prediction extrapolation [32].

2.7. TLR4 activation assay with HEK-Blue hTLR4 cells

HEK-Blue hTLR4 cells were cultured in DMEM high glucose medium supplemented with 10% fetal bovine serum (FBS), 2 mM glutamine, antibiotics and 1× HEK-Blue™ Selection (Invivogen). Cells were detached using a cell scraper, counted and seeded in a 96-well multiwell plate at a density of 4×10^4 cells per well. After overnight incubation (37 °C, 5% CO_2, 95% humidity), supernatants were replaced with only DMEM w/o Phenol Red. The activation assay was conducted stimulating cells with different concentrations (0.1, 1, 10, 100 ng/ml) of *A. pasteurianus* CIP103108 LPS or *E. coli* O55:B5 LPS (Sigma-Aldrich) for 16 h. While, the competition assay was performed pre-incubating cells with *A. pasteurianus* CIP103108 LPS (0.1, 1, 10, 100 ng/ml) for 30 min and then adding cells 1 ng/ml of *E. coli* O55:B5 LPS. After 16 h of incubation SEAP-containing supernatants were collected and incubated with paranitrophenylphosphate (pNPP) for 2–4 h in the dark at room temperature. The wells optical density (OD) was determined using a microplate reader set to 405 nm. Regarding activation assay, SEAP levels (OD at 405 nm) were used as indicator of TLR4 pathway activation. For the competition assay, data were normalized with respect to *E. coli* LPS stimulation and represented as fold decrease.

3. Results

3.1. LPS isolation, purification and compositional analysis

The LPS of *A. pasteurianus* CIP103108 was isolated using the hot phenol-water procedure [22]; DOC-PAGE analysis revealed the presence of a mixture of R-type LPS (the *O*-polysaccharide lacking form) and S-type LPS in the extract (Fig. S1). Purification steps, including enzymatic digestion followed by size exclusion chromatography in denaturing conditions, allowed to isolate S-type LPS and R-type LPS (Fig. S1). The sugar compositional analysis of the fraction containing S-LPS revealed the occurrence of L-rhamnose (Rha), D-mannose (Man), D-glucose (Glc), D-galactose (Gal), and, in minor amount, of D-glucuronic acid (GlcA), D-glucosamine (GlcN), 2,3-diamino-2-3-dideoxy-D-glucose (DAG), 3-deoxy-D-*manno*-oct-2-ulosonic acid (Kdo) and D-*glycero*-D-*talo*-oct-2-ulosonic acid (Ko). The sugar compositional analysis of isolated lipid A showed presence of GlcA, Man, GlcN, DAG and Ko. The compositional analysis in R-LPS revealed the presence of Rha, GlcA, Man, Glc, GlcN, DAG, Kdo and Ko. Methylation analysis of LPS [24] revealed the presence of 2,4-disubstituted Rha*p*, 2-substituted Rha*p*, 2-substituted Man*p*, terminal Glc*p*, 6-substituted-Glc*p* and 2,6-disubstituted and 3-substituted Gal*f*. The following fatty acids were also found: 14:0 (3-OH), 18:0 (3-OH) and 16:0. A selective *O*-deacylation [23] revealed presence of 14:0(3-OH) and 16:0, thus suggesting that 18:0 (3-OH) was the only *N*-linked acyl chain.

3.2. Isolation, purification of lipid A and O-polysaccharide fractions

An aliquot of pure S-LPS underwent a mild acid hydrolysis in order to separate the lipid A moiety from the sugar part, therefore the *O*-chain containing fraction was recovered and further purified using gel filtration chromatography. NMR spectra and compositional analysis revealed the presence of two polysaccharide containing fractions, **PS1** and **PS2** (Fig. 1). **PS2** was eluted first and thus possessed higher molecular mass compared to **PS1**. The two fractions were characterized as follows.

3.3. Structural characterization of *PS1* and *PS2*

The spin systems and monosaccharide sequence were characterized using a combination of 1D and 2D NMR spectra. The anomeric configuration of the monosaccharides were assigned on the basis of the $^3J_{H1,H2}$ and $^1J_{C1,H1}$ coupling constants and confirmed by the *intra*-residual NOE contacts; the vicinal $^3J_{H,H}$ coupling constants and *intra* residual NOE contacts revealed the relative configuration of the sugar residues.

The anomeric region of **PS1** revealed the presence of four different anomeric signals (Fig. 1a, Table 1). Spin systems **A**, **B** and **D** at 5.21, 5.07 and 4.97 ppm were identified as β-D-Gal*f* units. The downfield shift of all carbon signals, the strong downfield shift of carbon C-4 and the *intra*-residual long-range correlation between positions 1 and 4 found in the HMBC spectrum (Fig. 2) were diagnostic of a furanose ring [33]. The β-anomeric configuration was assessed on the basis of ^{13}C chemical shift [34]. Spin system **C** was identified as an α-D-Glc*p*; its anomeric configuration was assigned on the basis of $^1J_{C1,H1}$ (Table 1) and the $^3J_{H1,H2}$ (<4 Hz) whereas high $^3J_{H3,H4}$ (9.1 Hz) and intra-residual NOE connectivity of H-3 and H-5 confirmed the *gluco* configuration.

The downfield shift of carbon resonances suggested glycosylated positions at O-2 and O-6 of **A**, O-6 of **B** and O-3 of **D**. Spin system **C** was characterized as a terminal Glc residue. The *inter*-residual connectivity (Fig. S2) along with long-range correlations found on the HMBC spectrum (Fig. 2) of **A**1/**D**3, **B**1/**D**3, **D**1/**A**6 and **C**1/**A**2 allowed to define the saccharide sequence. Residue **C** was found to be not stoichiometrically linked at position O-2 of the galactofuranose residue **A,** substituted for about 75%.

A/B **D**
-6)-[D-Glc*p*-(α1-2)]-Gal*f*-(β1-3)-D-Gal*f*-(β1-
C*

**non-stoichiometric substitution*

The NMR spectrum of **PS2** unveiled the presence of five anomeric signals (Figs. 1b and 3, Table 2). Spin systems **A** and **B**, H-1 at 5.10 and 5.03 ppm respectively (Table 2), were characterized as α-rhamnopyranose units. In both cases, correlations of the ring protons with methyl signals were visible from the TOCSY spectrum. The *manno* configuration of both spin systems was assigned on the basis of $^3J_{H1,H2}$ and $^3J_{H2,H3}$ coupling constants, the α-configuration from *intra*-residual NOE contact of H-1 with H-2 and the chemical shift value of C-5. Analogously, spin systems **C** and **D** were assigned as α-glucopyranose units while spin system **E** was identified as α-mannopyranose. The downfield shift of carbon resonances identified the glycosylated positions: O-2 and O-4 of **A**, O-2 of **B,** O-6 of **D** and O-2 of **E**. Unit **C** was identified as a terminal residue. The *inter*-residual NOE contacts observed from the ROESY spectrum (Fig. S3) together with the long-range correlations, derived from the HMBC spectrum (Fig. 3), between **A**1 with **E**2; **E**1 with **D**6, **D**1 with **B**2; **B**1 with **A**2 so as **C**1 with **A**4 confirmed the following repeating unit for the polysaccharide **PS2**:

C
-6)-D-Glc*p*-(α1-2)-L-Rha*p*-(α1-2)-[Glc*p*-(α1-4)]-L-Rha*p*-(α1-2)-D-Man*p*-(α1-
D **B** **A** **E**

3.4. MALDI MS on A. pasteurianus CIP103108 lipid A

A. pasteurianus CIP103108 lipid A structure was investigated by MALDI-MS and MS/MS. The negative-ion MALDI MS spectrum (Fig. 4) revealed the presence of several cluster of peaks in the mass range *m/z* 1543.9–2434.7, indicative of lipid A species with a different acylation degree. Each cluster was characterized by the presence of mass differences of 14 amu (–CH_2– unit), attributable to lipid A species differing by the length of their acyl chains (Fig. 4).

In detail and based on the compositional analysis, cluster of peaks at around *m/z* 2406.7 matched with hexa-acylated lipid A species with a pentasaccharide sugar backbone containing one hexose (identified as Man), one DAG, one GlcN, one acid (identified as GlcA) and one Ko

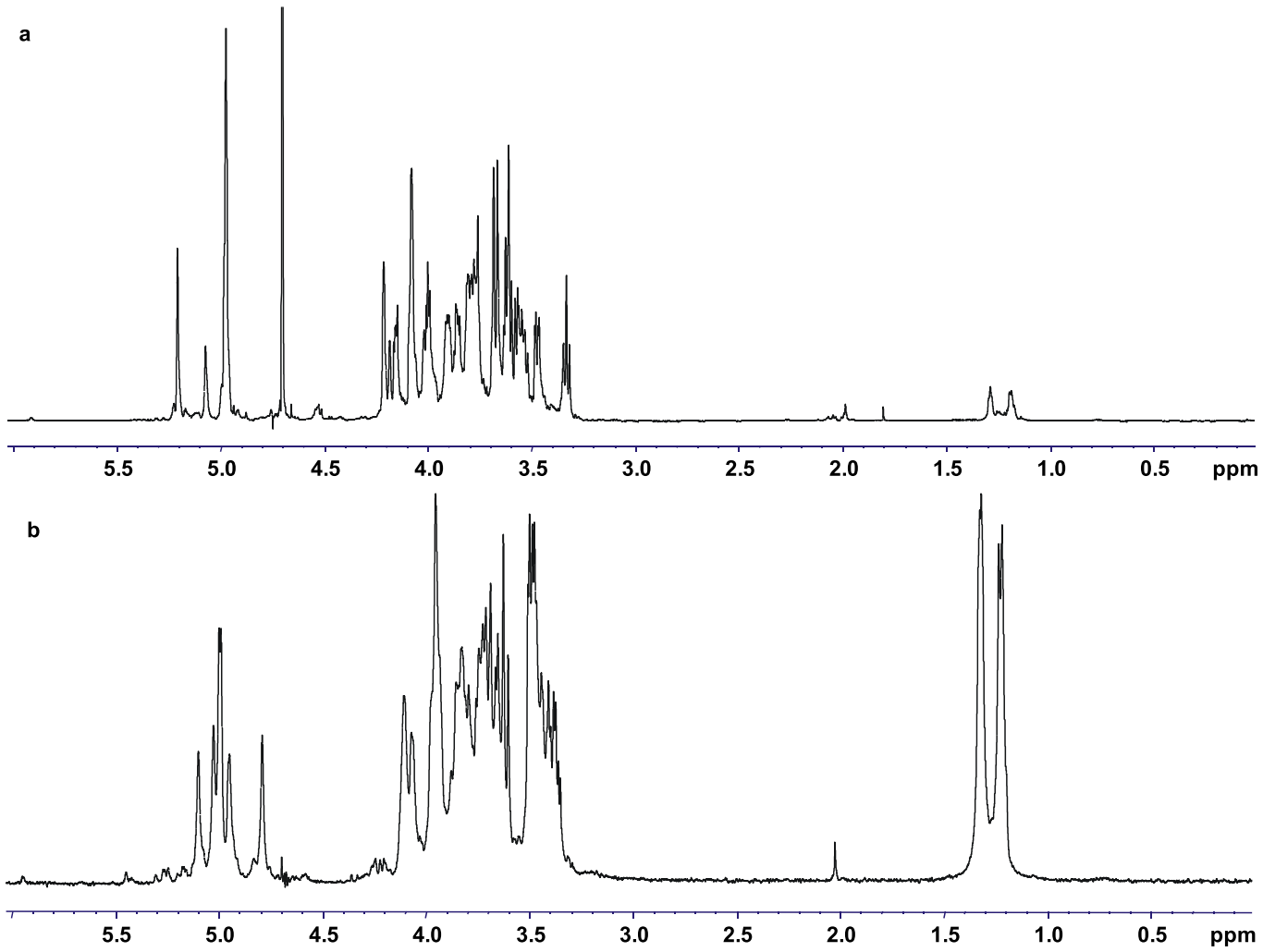

Fig. 1. ^{1}H NMR spectra of (a) **PS1** and (b) **PS2.**

unit and acylated by two 14:0 (3-OH), two 18:0 (3-OH) and two 16:0, in accordance with previously reported structure on *A. pasteurianus* NBRC 3283 lipid A [35]. The cluster at *m/z* 2168.4 was assigned to penta-acylated lipid A species made up of two 14:0 (3-OH), two 18:0 (3-OH) and one 16:0, thereafter, tetra-acylated lipid A species at *m/z* 1942.2, devoid of one 14:0 (3-OH) with respect to the species at *m/z* 2168.4, was also identified. Furthermore, tetra-acylated species lacking one hexose and/or Ko units and minor tri-acylated species were also present in the MALDI spectrum (Fig. 4).

MS/MS experiments were performed in order to characterize the location of the lipid A acyl chains with respect to the saccharide backbone [26,36]. The negative-ion MS/MS spectrum of precursor ion *m/z* 1942.2 (Fig. S4 and S5), consistent with a tetra-acylated pentasaccharidic species, showed an intense peak at *m/z* 1706.1 attributed to an ion originated from the loss of Ko residue. Peaks at *m/z* 1766.1 and 1780.1 were assigned to fragments lacking the GlcA and the hexose unit respectively. A lipid A fragment devoid of the 16:0 moiety was attributed to the peak at *m/z* 1686.1. More importantly, peaks originating from the sugar ring fragmentations $^{1,3}A_3$ (*m/z* 1582.5), $^{1,4}A_3$ (*m/z* 1552.5), $^{0,3}A_3$ (*m/z* 1393.3) and $^{0,4}A_3$ (*m/z* 1362.4) were very informative as they clearly demonstrated that the proximal GlcN was decorated by a GlcA and an amide-bound 18:0 (3-OH) moiety whereas the distal DAG was substituted by Ko, hexose and acylated by one 18:0 (3-OH), one 14:0 (3-OH) and one secondary 16:0 fatty acid. Finally, the peak at *m/z* 1450.0 was ascribed to a fragment ion where both Ko and 16:0 were absent.

MS/MS experiments conducted on precursor ion at *m/z* 2168.4 (Fig. S6) showed an ion peak at *m/z* 1932.3 originating from the loss of Ko unit, as well as from the loss of the hexose at *m/z* 2006.3. Lipid A fragments lacking the Ko and one 14:0 (3-OH) (*m/z* 1688.2) and one 16:0 (m/z 1432.3) were also identified. Moreover, ions originated from the loss of the hexose unit and 16:0 (*m/z* 1750.3) and from the loss of the hexose and one 14:0 (3-OH) (*m/z* 1762.3) were also detected. The absence of an ion originating from the loss of a whole hydroxylated 18:0 or 14:0 bearing a 16:0 suggested that the secondary fatty acid was linked to the acyloxyacyl amides, thus excluding its presence on the proximal GlcN as a substituent of the primary ester-bound 14:0 (3-OH). Furthermore, in support of this hypothesis, a peak was found at

Table 1
Proton (^{1}H) and carbon (^{13}C) (*italic*) NMR shifts of *A. pasteurianus* CIP103108 **PS1.**

Residue	1	2	3	4	5	6
A	5.21	4.08	4.15	3.86	3.91	3.53/3.78
2,6-β-D-Gal*f*	*105.2*	*86.6*	*75.0*	*82.3*	*69.0*	*69.3*
	$^{1}J_{C1,H1}$ 172.3 Hz	$^{3}J_{H1,H2}$ 3.4 Hz	$^{3}J_{H2,H3}$ 9.5 Hz	$^{3}J_{H3,H4}$ 9.4 Hz	$^{3}J_{H4,H5}$ 9.4 Hz	
B	5.07	4.02	3.97	3.84	3.86	3.77/3.50
6-β-D-Gal*f*	*106.8*	*81.2*	*76.6*	*82.9*	*69.2*	*69.3*
C	4.98	3.47	3.61	3.34	3.67	3.77/3.67
t-α-D-Glc*p*	*98.1*	*71.1*	*72.7*	*69.4*	*72.3*	*60.4*
D	4.97	4.21	4.09	4.00	3.80	3.62/3.57
3-β-D-Gal*f*	*108.1*	*79.2*	*82.6*	*82.0*	*70.7*	*62.7*

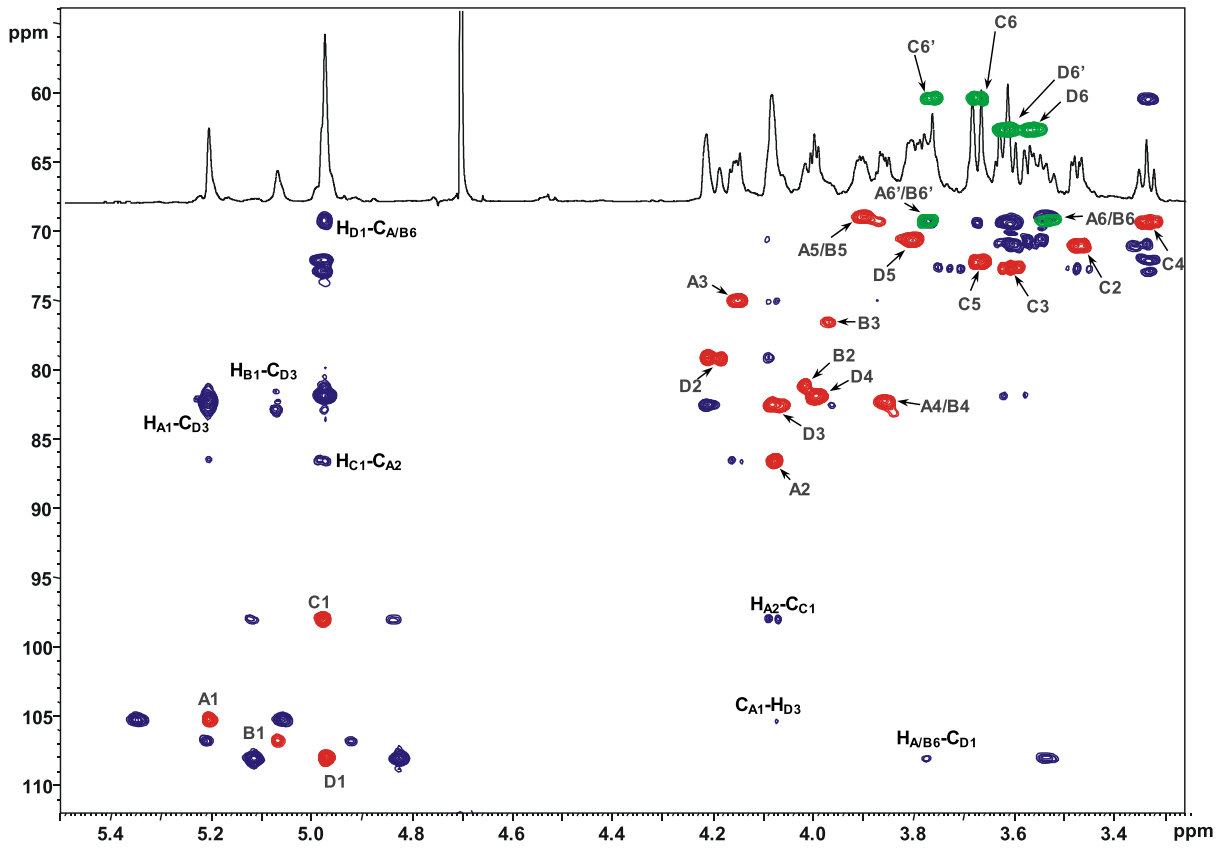

Fig. 2. Overlapped sections of ^{1}H ^{13}C HMBC (blue) and ^{1}H ^{13}C HSQC (red and green) NMR of **PS1**. The anomeric signals and key *inter*-residual long range correlations involving sugar residues of **PS1** are indicated. Letters are as found in Table 1.

m/z 1984.4 resulting from the loss of 184 amu arising from the primary *O*-linked 14:0 (3-OH) and promoted by its free 3-OH group. Unfortunately, no ions originating from sugar ring fragmentations were detected. In addition, MS/MS spectrum of precursor ion at *m/z* 2406.7 (Fig. S7), relative to a hexa-acylated lipid A species, presented the ion peak derived from the sugar ring fragmentation $^{1,4}A_3$ at *m/z* 1791.5 that was fundamental to further corroborate the location of the 16:0 residues as secondary acyl substituents of the DAG unit.

Therefore, the lipid A and O-chain structure from *A. pasterianus CIP103108* were as reported in Fig. 5.

3.5. Immunological studies on A. pasterianus CIP103108 LPS

Studies on immunological properties of *A. pasterianus* CIP103108 LPS were performed using HEK-Blue hTLR4 cells. These cells are designed for studying the activation of human TLR4 by monitoring the activation of NF-κB and AP-1 transcription factors. HEK-Blue hTLR4 cells are HEK cells transfected in order to stably express hTLR4, hMD-2 and hCD14 receptor genes and a secreted embryonic alkaline phosphatase (SEAP) reporter gene placed under the control of NF-κB and AP-1. Stimulation with a TLR4 ligand activates NF-κB and AP-1 inducing the production and secretion of SEAP in cells culture medium. Levels of SEAP can be easily determined incubating the enzyme with *para*-nitrophenylphosphate (pNPP). In order to evaluate the capacity of *A. pasteurianus* CIP 103108 LPS to trigger TLR4-mediated signalling (activation assay) cells were exposed to different concentrations (0.1, 1, 10, 100 ng/ml) of this LPS variant for 16 h. As a positive control *E. coli* O55:B5 LPS was used. As expected, *E. coli* O55:B5 LPS strongly activated TLR4-mediated pathway in a dose-dependent manner. On the contrary, the results obtained revealed that *A. pasteurianus* CIP103108 LPS was incapable to trigger the activation of the same pathway (Fig. S8A). Furthermore, the capability of *A. pasteurianus* CIP103108 LPS to interfere with *E. coli* LPS-triggered TLR4-mediated signalling was also evaluated (competition assay). To investigate this aspect, cells were pre-incubated with different concentration of *A. pasteurianus* CIP103108 LPS (0.1, 1, 10, 100 ng/ml) for 30 min and then exposed to *E. coli* O55:B5 LPS (1 ng/ml) for 16 h. Results showed that the pre-incubation with *A. pasteurianus* CIP103108 LPS slightly reduced the capacity of cells to respond to *E. coli* O55:B5 LPS, as demonstrated by the minor activation of the TLR4-mediated pathway (Fig. S8 B).

4. Discussion

In this work we have focused our attention on the structural characterization of the LPS isolated from *A. pasteurianus* CIP103108. Two novel LPS O-chains were found, **PS1** and **PS2**, both possessing structural analogies with those isolated from other *Acetobacter* strains. The presence of two different O-chains is not considered as a common feature of LPSs, nevertheless this phenomenon was reported among *Burkholderia* species [37]. **PS1** possessed a Gal*f* disaccharide repeating unit carrying a non-stoichiometric Glc substitution; it showed subtle compositional similarities with the O-chains isolated from two *Acetobacter methanolicus* strains, MB58/4 [38] and MB70 [39]. Moreover, we have also found that a similar exopolysaccharide was produced by another acidophilic bacterium, *Zymomonas mobilis*, which was proven to have relevance with the outer milieu of bacterium (manuscript in preparation). The second polysaccharide **PS2** contained a pentasaccharide repeating unit constituted by a tetrasaccharide skeleton containing glucose, mannose and two rhamnose residues, one of which carrying a terminal glucose as an appendage. A similar O-antigen was reported for *Acetobacter tropicalis* SKU1100 [40], whose backbone also contained two rhamnose residues, although in an α-(1–3) linkage, instead of the α-(1–2) here reported, with one rhamnose further substituted by a glucose residue. Furthermore, other O-

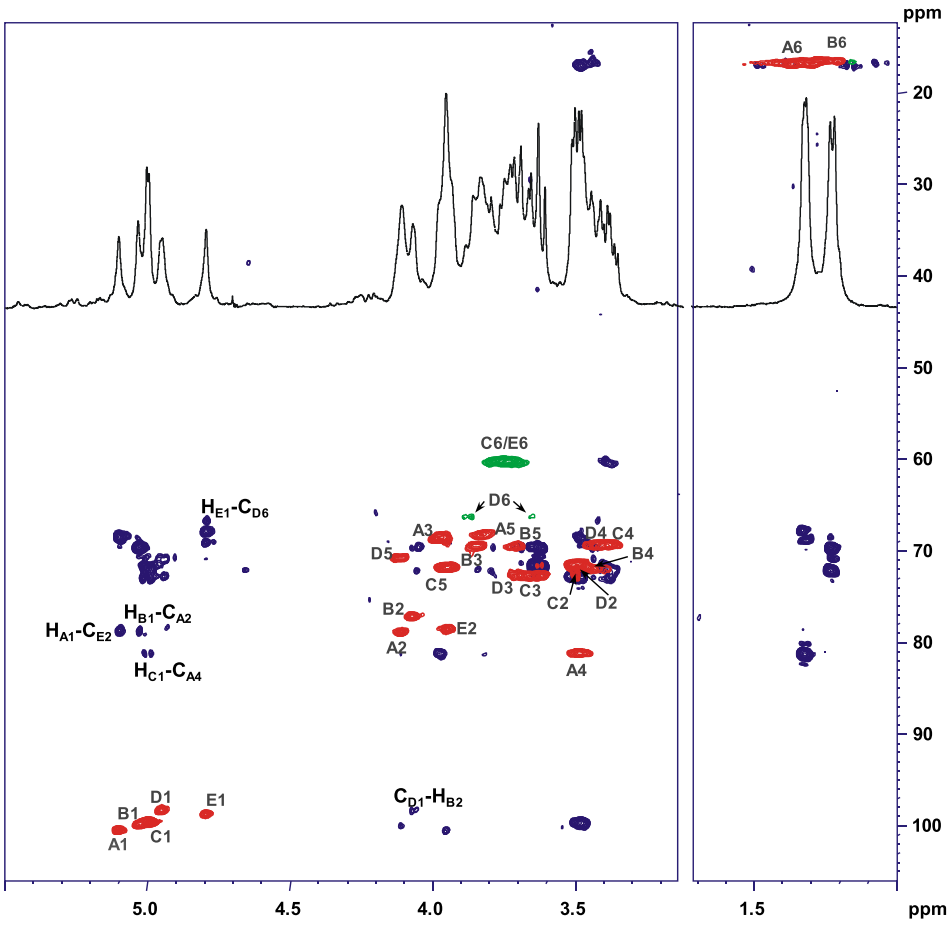

Fig. 3. Overlapped sections of ^{1}H ^{13}C HMBC (blue) and ^{1}H—^{13}C HSQC (red and green) NMR of **PS2**. The anomeric signals and key *inter*-residual long range correlations involving sugar residues of **PS2** are indicated. Letters found in Table 2.

polysaccharides possessing structural similarities were also found in *Acetobacter diazotrophicus* PAL5 [41]. None of the above structures possessed mannose residues, though for *A. diazotrophicus* PAL5 contained a *manno*-configured sugar.

Recently, Hashimoto et al. [35] reported about the capability of *A. pasteurianus* NBRC 3283 LPS to remain stable in acidic conditions for long periods and correlated this capability to its unique lipid A structure.

Table 2
Values of ^{1}H and ^{13}C (*italic*) chemical shifts of *A. pasteurianus* CIP103108 **PS2.**

Residue	1	2	3	4	5	6
A	5.10	4.11	3.97	3.49	3.82	1.32
2,4-α-L-Rha*p*	*100.5*	*78.9*	*68.6*	*81.2*	*68.3*	*16.9*
	$^{1}J_{C1,H1}$ 173.4 Hz	$^{3}J_{H1,H2}$< 1 Hz	$^{3}J_{H2,H3}$ 2.4 Hz	$^{3}J_{H3,H4}$ 9.02 Hz		
B	5.03	4.07	3.84	3.45	3.71	1.22
2-α-L-Rha*p*	*99.9*	*77.3*	*69.6*	*72.0*	*69.6*	*16.6*
	$^{1}J_{C1,H1}$ 172.0 Hz	$^{3}J_{H1,H2}$ < 1 Hz	$^{3}J_{H2,H3}$ 3.0 Hz	$^{3}J_{H3,H4}$ 9.5 Hz		
C	5.00	3.49	3.63	3.39	3.94	3.75
t-α-D-Glc*p*	*99.6*	*71.5*	*72.8*	*69.5*	*71.9*	*60.2*
	$^{1}J_{C1,H1}$ 174.4 Hz	$^{3}J_{H1,H2}$ 3.5 Hz	$^{3}J_{H2,H3}$ 9.4 Hz	$^{3}J_{H3,H4}$ 9.5 Hz		
D	4.95	3.50	3.69	3.43	4.10	3.65/3.88
6-α-D-Glc*p*	*98.3*	*71.5*	*72.8*	*69.5*	*70.8*	*66.4*
	$^{1}J_{C1,H1}$ 174.2 Hz	$^{3}J_{H1,H2}$ 2.9 Hz	$^{3}J_{H2,H3}$ 9.5 Hz	$^{3}J_{H3,H4}$ 9.6 Hz		
E	4.80	3.95	3.84	3.38	3.63	3.76
2-α-D-Man*p*	*98.7*	*78.6*	*67.9*	*69.4*	*69.2*	*60.2*
	$^{1}J_{C1,H1}$ 173.2 Hz	$^{3}J_{H1,H2}$ < 1 Hz	$^{3}J_{H2,H3}$ 3.5 Hz	$^{3}J_{H3,H4}$ 9.5 Hz		

Indeed, the authors demonstrated that the LPS was characterized by the occurrence of a D-*glycero*-D-*talo*-oct-2-ulosonic acid (Ko), in place of Kdo, as the first sugar of the core OS, directly linked to the lipid A domain. This was explained with the acid-lability of Kdo that would be degraded in the acid environmental conditions of bacterium life. Thus, the substitution of Kdo with the acid-stable Ko is considered as an adaptation phenomenon necessary for bacterial survival. The presence of Ko has been so far described in the core oligosaccharides from *Burkholderia*, *Acinetobacter*, *Yersinia*, and *Serratia* species [42], although a direct linkage of Ko to the lipid A has so far reported only for *Acinetobacter haemolyticus* [43], in which the Kdo is almost completely replaced by Ko residues. Furthermore, *A. pasteurianus* LPS is devoid of phosphate groups and the lipid A is characterized by tetrasaccharide backbone composed of Man-DAG-GlcN-GlcA. Interestingly, lipid A devoid of phosphate groups and with a similar sugar skeleton were already reported for other plant associated bacteria belonging to the *Alphaproteobacteria* family, as *Rhizobiaceae* and *Bradyrhizobiaceae*. The lipid A isolated from *Rhodopseudomonas palustris* [19] possessed nearly the same tetrasaccharide skeleton but with a complete DAG skeleton. *Bradyrhizobium* strains possess instead an α-(1 → 6)-mannose disaccharide linked to the non-reducing DAG [44,45]. Moreover, a DAG-GlcN disaccharide skeleton was previously reported for *Campylobacter jejuni* [46] while a DAG backbone has been found in the lipid A of other strains like *Azorhizobium caulinodans* [47], *Phyllobacterium trifolii* [48], *Leptospira interrogans* [49], *Acidithiobacillus ferrooxidans* [50], *Thiobacillus* [51], *Bartonella* [21] and *Brucella* [52]. The occurrence of this phenomenon is explained by the presence of two enzymes, GnnA and GnnB in the lipid A biosynthesis process which are pivotal for synthesis of UDP-D-Glc*p*N3N from UDP-D-Glc*p*NAc [53].

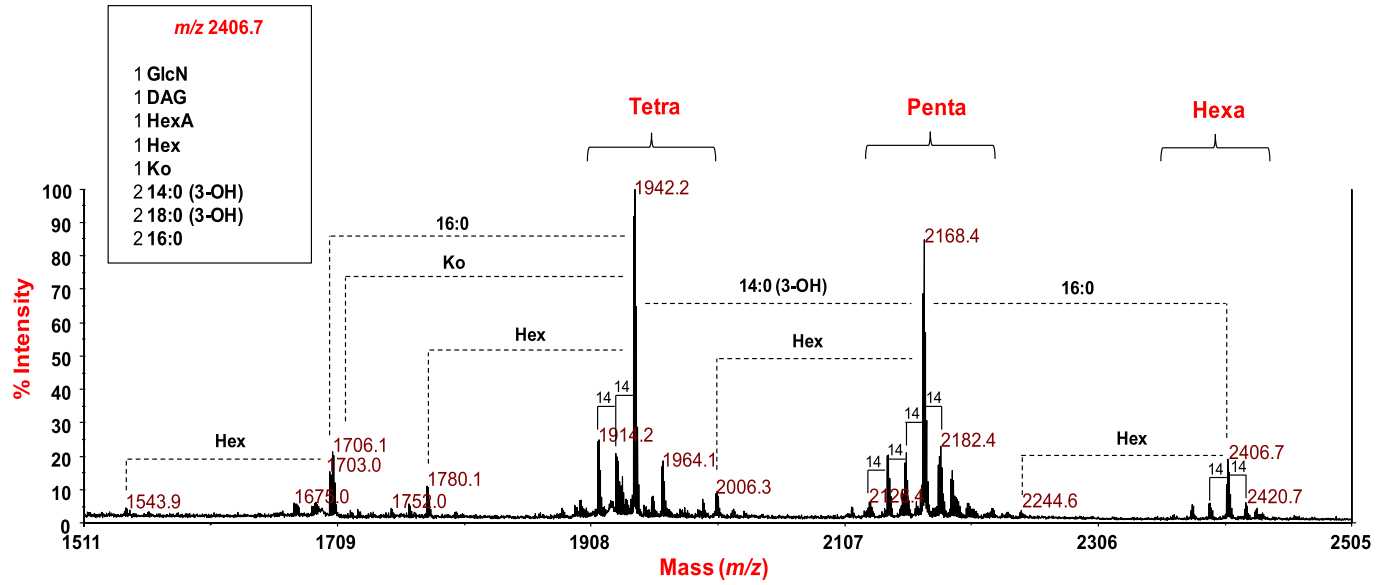

Fig. 4. Reflectron MALDI mass spectrum, recorded in negative polarity, of the *A. pasteurianus* CIP103108 lipid A. Lipid A species are outlined. In the inset, the proposed structural composition of the peak at *m/z* 2406.7 is listed.

The lipid A is considered as the center of toxicity of the LPS. It is well known that this part of the molecule is recognized by the TLR4/MD-2 receptor complex resulting in immunostimulation activity. A widely known fact is that hexa-acylated *bis*-phosphorylated lipid A produced by *E. coli* possesses high affinity to TLR4/MD-2 receptor complex, triggering powerful innate immune response. Overstimulation by agonistic LPS can deregulate innate immune system signalling, finally effecting in uncontrolled, massive proinflammatory cytokine release. Nevertheless, it was shown that modifications of the lipid A structure can tune and modulate the innate immune response. Within this frame, research and investigation of natural LPS able to inhibit the TLR4/MD-2 dependent signalling is an important and interesting topic.

The results obtained on TLR4/MD-2 mediated NF-kB activation on *A. pasteurianus* CIP103108 LPS have shown significantly lower response than *E. coli* O55:B5 LPS. A weak effect of inhibition of the TLR4/MD-2 mediated activation of NF-kB induced by *E. coli* O55:B5 LPS was also observed. The very weak agonist activity may be explained by lipid A structural features as i) the absence of phosphate groups [54], ii) the presence of penta-, tetra- and tri-acylated species, besides the hexa-acylated form, iii) the occurrence of a DAG unit.

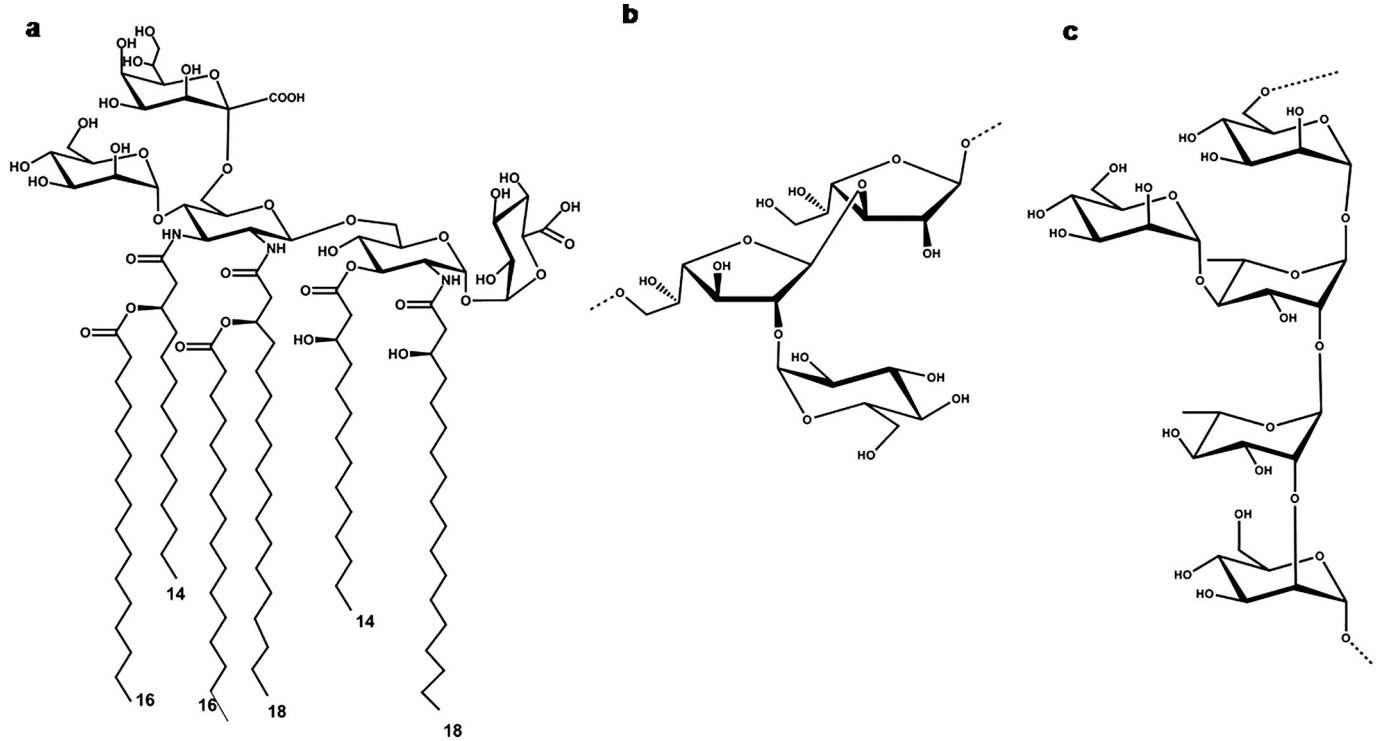

Fig. 5. Structure of the a) lipid A and two O-polysaccharides, b) **PS1** c) **PS2** isolated from *Acetobacter pasteurianus* CIP103108.

Acknowledgements

AS, AM, FP and MP acknowledge the European Commission (H2020-MSCA-ETN-642157 TOLLerant project).

Appendix A. Supplementary data

Supplementary data to this article can be found online at https://doi.org/10.1016/j.ijbiomac.2018.08.035.

References

[1] M.P. Doyle, L.R. Steenson, Bacteria in Food and Beverage Production, in: J. Meng, E. Rosenberg, E.F. DeLong, S. Lory, E. Stackebrandt, F. Thompson (Eds.), The Prokaryotes, Springer, Berlin, Heidelberg 2013, pp. 241–256.
[2] I.Y. Sengun, S. Karabiyikli, Importance of acetic acid bacteria in food industry, Food Control 22 (5) (2011) 647–656.
[3] Y. Yamada, P. Yukphan, Genera and species in acetic acid bacteria, Int. J. Food Microbiol. 125 (1) (2008) 15–24.
[4] K. Nanda, M. Taniguchi, S. Ujike, N. Ishihara, H. Mori, H. Ono, Y. Murooka, Characterization of acetic acid bacteria in traditional acetic acid fermentation of rice vinegar (*komesu*) and unpolished rice vinegar (*kurosu*) produced in Japan, Appl. Environ. Microbiol. 67 (2001) 986–990.
[5] M. Hashimoto, T. Matsumoto, M. Tamura-Nakano, M. Ozono, S. Hashiguchi, Y. Suda, Characterization of outer membrane vesicles of *Acetobacter pasteurianus* NBRC3283, J. Biosci. Bioeng. 125 (4) (2017) 425–431.
[6] M. Hashimoto, K. Obara, M. Ozono, M. Furuyashiki, T. Ikeda, Y. Suda, K. Fukase, Y. Fujimoto, H. Shigehisa, Separation and characterization of the immunostimulatory components in unpolished rice black vinegar (*kurozu*), J. Biosci. Bioeng. 116 (6) (2013) 688–696.
[7] X. Wang, P.J. Quinn, Endotoxins: lipopolysaccharides of gram-negative bacteria, in: X. Wang, P.J. Quinn (Eds.), Endotoxins: Structure, Function and Recognition, Subcellular Biochemistry, 53, Springer, Dordrecht Heidelberg London New York 2010, pp. 3–25.
[8] A. Molinaro, O. Holst, F. Di Lorenzo, M. Callaghan, A. Nurisso, G. D'Errico, A. Zamyatina, F. Peri, R. Berisio, R. Jerala, J. Jiménez-Barbero, A. Silipo, S. Martín-Santamaría, Chemistry of lipid A: at the heart of innate immunity, Chem. Eur. J. 21 (2) (2015) 500–519.
[9] F. Di Lorenzo, J.M. Billod, S. Martín-Santamaría, A. Silipo, A. Molinaro, Gram negative extremophile lipopolysaccharides: promising source of inspiration for a new generation of endotoxin antagonists, Eur. J. Org. Chem. (2017) 4055–4073.
[10] A. Silipo, A. Molinaro, The diversity of the core oligosaccharide in lipopolysaccharides, in: X. Wang, P.J. Quinn (Eds.), Endotoxins: Structure, Function and Recognition, Sub-cellular Biochemistry, 53, Springer, Dordrecht Heidelberg London New York 2010, pp. 69–99.
[11] M. Caroff, D. Karibian, Structure of bacterial lipopolysaccharides, Carbohydr. Res. 338 (23) (2003) 2431–2447.
[12] C.R. Raetz, C. Whitfield, Lipopolysaccharide endotoxins, Annu. Rev. Biochem. 71 (2002) 635–700.
[13] K. Miyake, Innate recognition of lipopolysaccharide by Toll-like receptor 4–MD-2, Trends Microbiol. 12 (4) (2004) 186–192.
[14] B.S. Park, J.O. Lee, Recognition of lipopolysaccharide pattern by TLR4 complexes, Exp. Mol. Med. 6 (2013) 45–66.
[15] H. Loppnow, P. Libby, M. Freudenberg, J.H. Krauss, J. Weckesser, H. Mayer, Cytokine induction by lipopolysaccharide (LPS) corresponds to lethal toxicity and is inhibited by nontoxic *Rhodobacter capsulatus* LPS, Infect. Immun. 58 (11) (1990) 3743–3750.
[16] S. Saitoh, S. Akashi, T. Yamada, N. Tanimura, M. Kobayashi, K. Konno, F. Matsumoto, K. Fukase, S. Kusumoto, Y. Nagai, Y. Kusumoto, A. Kosugi, K. Miyake, Lipid A antagonist, lipid IVa, is distinct from lipid A in interaction with Toll-like receptor 4 (TLR4)-MD-2 and ligand-induced TLR4 oligomerization, Int. Immunol. 16 (7) (2004) 961–969.
[17] P.M. Lepper, M. Triantafilou, C. Schumann, E.M. Schneider, K. Triantafilou, Lipopolysaccharides from *Helicobacter pylori* can act as antagonists for Toll-like receptor 4, Cell. Microbiol. 7 (4) (2005) 519–528.
[18] F. Di Lorenzo, A. Palmigiano, I. Paciello, M. Pallach, D. Garozzo, M.L. Bernardini, V. Cono, M.M. Yakimov, A. Molinaro, A. Silipo, The deep-sea Polyextremophile *Halobacteroides lacunaris* TB21 rough-type LPS: structure and inhibitory activity towards toxic LPS, Mar. Drugs 15 (7) (2017) 201.
[19] F. Di Lorenzo, A. Palmigiano, S. Al Bitar-Nehme, L. Sturiale, K.A. Duda, D. Gully, R. Lanzetta, E. Giraud, D. Garozzo, M.L. Bernardini, A. Molinaro, A. Silipo, The lipid A from *Rhodopseudomonas palustris* strain BisA53 LPS possesses a unique structure and low immunostimulant properties, Chem. Eur. J. 23 (7) (2017) 3637–3647.
[20] A. Ialenti, P. Di Meglio, G. Grassia, P. Maffia, M. Di Rosa, R. Lanzetta, A. Molinaro, A. Silipo, W.D. Grant, A. Ianaro, A novel lipid A from. *Halomonas magadiensis* inhibits enteric LPS-induced human monocyte activation, Eur. J. Immunol. 36 (2) (2006) 354–360.
[21] G. Malgorzata-Miller, L. Heinbockel, K. Brandenburg, J.W.M. Van der Meer, M.G. Netea, L.A.B. Joostena, *Bartonella quintana* lipopolysaccharide (LPS): structure and characteristics of a potent TLR4 antagonist for in-vitro and in-vivo applications, Sci. Rep. 6 (2016) 34221.
[22] O. Westphal, K. Jann, Bacterial lipopolysaccharides. Extraction with phenol water and further applications of the procedure, in: R.L. Whistler (Ed.), Methods in Carbohydrate Chemistry, Academic, New York, NY 1965, pp. 83–91.
[23] C. De Castro, M. Parrilli, O. Holst, A. Molinaro, Microbe-associated molecular patterns in innate immunity: extraction and chemical analysis of gram-negative bacterial lipopolysaccharides, Methods Enzymol. 480 (2010) 89–115.
[24] I. Ciucanu, F. Kerek, A simple and rapid method for the permethylation of carbohydrates, Carbohydr. Res. 131 (1984) 209–217.
[25] E.G. Bligh, W.J. Dyer, A rapid method of total lipid extraction and purification, Can. J. Biochem. Physiol. 37 (1959) 911–917.
[26] A. Silipo, L. Sturiale, D. Garozzo, C. De Castro, R. Lanzetta, M. Parrilli, W.D. Grant, A. Molinaro, Structure elucidation of the highly heterogeneous lipid a from the lipopolysaccharide of the gram-negative extremophile bacterium *Halomonas magadiensis* Strain 21 M1, Eur. J. Org. Chem. 10 (2004) 2263–2271.
[27] F. Di Lorenzo, The lipopolysaccharide lipid A structure from the marine sponge-associated bacterium *Pseudoalteromonas* sp. 2A, A. Van. Leeuw. J. Microb. 110 (11) (2017) 1401–1412.
[28] L. Sturiale, A. Palmigiano, A. Silipo, Y.A. Knirel, A.P. Anisimov, R. Lanzetta, M. Parrilli, A. Molinaro, D. Garozzo, Reflectron MALDI TOF and MALDI TOF/TOF mass spectrometry reveal novel structural details of native lipooligosaccharides, J. Mass Spectrom. 46 (2011) 1135–1142.
[29] U. Piantini, O.W. Sorensen, R.R. Ernst, Multiple quantum filters for elucidating NMR coupling networks, J. Am. Chem. Soc. 104 (1982) 6800–6801.
[30] M. Rance, O.W. Sørensen, G. Bodenhausen, G. Wagner, R.R. Ernst, K. Wüthrich, Improved spectral resolution in COSY ^{1}H NMR spectra of proteins via double quantum filtering, Biochem. Biophys. Res. Commun. 117 (1983) 479–485.
[31] D.J. States, R.A. Haberkorn, D.J. Ruben, A two-dimensional nuclear Overhauser experiment with pure absorption phase in four quadrants, J. Magn. Reson. 48 (1982) 286–292.
[32] A.S. Stern, K.B. Li, J.C. Hoch, Modern spectrum analysis in multidimensional NMR spectroscopy: comparison of linear-prediction extrapolation and maximum-entropy reconstruction, J. Am. Chem. Soc. 124 (2002) 1982–1993.
[33] F. Di Lorenzo, I. Paciello, L.L. Fazio, L. Albuquerque, L. Sturiale, M.S. Da Costa, R. Lanzetta, M. Parrilli, D. Garozzo, M.L. Bernardini, A. Silipo, A. Molinaro, Thermophiles as potential source of novel endotoxin antagonists: the full structure and bioactivity of the lipo-oligosaccharide from *Thermomonas hydrothermalis*, Chembiochem 15 (2014) 2146–2155.
[34] A. Molinaro, V. Piscopo, R. Lanzetta, M. Parrilli, Structural determination of the complex exopolysaccharide from the virulent strain of *Cryphonectria parasitica*, Carbohydr. Res. 337 (19) (2002) 1707–1713.
[35] M. Hashimoto, M. Ozono, M. Furuyashiki, R. Baba, S. Hashiguchi, Y. Suda, K. Fukase, Y. Fujimoto, Characterization of a novel D-*Glycero*-D-*talo*-oct-2-ulosonic acid-substituted lipid A moiety in the lipopolysaccharide produced by the acetic acid bacterium *Acetobacter pasteurianus* NBRC 3283, J. Biol. Chem. 291 (40) (2016) 21184–21194.
[36] L. Sturiale, D. Garozzo, A. Silipo, R. Lanzetta, M. Parrilli, A. Molinaro, New conditions for matrix assisted laser desorption/ionization mass spectrometry of native bacterial R-type lipopolysaccharides, Rapid Commun. Mass Spectrom. 19 (2005) 1829–1834.
[37] A.D. Vinion-Dubiel, J.B. Goldberg, Lipopolysaccharide of *Burkholderia cepacia* complex, J. Endotoxin Res. 9 (2003) 201–213.
[38] H.D. Grimmecke, U. Mamat, W. Lauk, A.S. Shashkov, Y.A. Knirel, E.V. Vinogradov, N.K. Kochetkov, Structure of the capsular polysaccharide and the O-side-chain of the lipopolysaccharide from *Acetobacter methanolicus* MB 58/4 (IMET 10945), and of oligosaccharides resulting from their degradation by the bacteriophage Acml, Carbohydr. Res. 220 (1991) 165–172.
[39] H.D. Grimmecke, Y.A. Knirel, A.S. Shashkov, B. Kiesel, W. Lauk, M. Voges, Structure of the capsular polysaccharide and the O-side-chain of the lipopolysaccharide from *Acetobacter methanolicus* MB 70, and of oligosaccharides resulting from their degradation by the bacteriophage Acm6, Carbohydr. Res. 253 (1994) 277–282.
[40] I.A.I. Ali, Y. Akakabe, S. Moonmangmee, A. Deeraksa, M. Matsutani, T. Yakushi, M. Yamada, K. Matsushita, Structural characterization of pellicle polysaccharides of *Acetobacter tropicalis* SKU1100 wild type and mutant strains, Carbohyd. Polym. 86 (2) (2011) 1000–1006.6.
[41] J.O. Previato, C. Jones, M.P. Stephan, L.P.A. Almeida, L. Mendonca-Previato, Structure of the repeating oligosaccharide from the lipopolysaccharide of the nitrogen-fixing bacterium *Acetobacter diazotrophicus* strain PAL 5, Carbohyd. Res. 298 (1997) 311–318.
[42] O. Holst, Structure of the Lipopolysaccharide Core Region, in: Y.A. Knirel, M.A. Valvano (Eds.), Bacterial Lipopolysaccharides, Springer-Verlag, Wien 2011, pp. 21–39.
[43] E.V. Vinogradov, S. Müller-Loennies, B.O. Petersen, S. Meshkov, J.E. Thomas-Oates, O. Holst, H. Brade, Structural investigation of the lipopolysaccharide from *Acinetobacter haemolyticus* strain NCTC 10305 (ATCC 17906, DNA group 4), Eur. J. Biochem. 247 (1) (1997) 82–90.
[44] A. Silipo, G. Vitiello, D. Gully, L. Sturiale, C. Chaintreuil, J. Fardoux, D. Gargani, H.I. Lee, G. Kulkarni, N. Busset, R. Marchetti, A. Palmigiano, H. Moll, R. Engel, R. Lanzetta, L. Paduano, M. Parrilli, W.S. Chang, O. Holst, D.K. Newman, D. Garozzo, G. D'Errico, E. Giraud, A. Molinaro, Covalently linked hopanoid-lipid a improves outer-membrane resistance of a *Bradyrhizobium* symbiont of legumes, Nat. Commun. 5 (2014) 5106.
[45] I. Komaniecka, A. Choma, B. Lindner, O. Holst, The structure of a novel neutral lipid a from the lipopolysaccharide of *Bradyrhizobium elkanii* containing three mannose units in the backbone, Chem. Eur. J. 16 (2010) 2922–2929.
[46] A. Van Mourik, L. Steeghs, J. Van Laar, H.D. Meiring, H.J. Hamstra, J.P.M. Van Putten, M.S.M. Wösten, Altered linkage of Hydroxyacyl chains in lipid a of *Campylobacter jejuni* reduces TLR4 activation and antimicrobial resistance, J. Biol. Chem. 285 (21) (2010) 15828–15836.

[47] A. Choma, I. Komaniecka, A. Turska-Szewczuk, W. Danikiewicz, G. Spolnik, Structure of lipid a from a stem-nodulating bacterium *Azorhizobium caulinodans*, Carbohydr. Res. 352 (2012) 126–136.
[48] K. Zamlynska, I. Komaniecka, K. Zebracki, A. Mazur, A. Sroka-Bartnicka, A. Choma, Studies on lipid a isolated from *Phyllobacterium trifolii* PETP02^{T} lipopolysaccharide, A. Van Leeuw. J. Microb. 110 (2017) 1413–1433.
[49] N.L. Que-Gewirth, A.A. Ribeiro, S.R. Kalb, R.J. Cotter, D.M. Bulach, B. Adler, I.S. Girons, C. Werts, C.R. Raetz, A methylated phosphate group and four amide-linked acyl chains in Leptospira interrogans lipid a the membrane anchor of an unusual lipopolysaccharide that activates TLR2, J. Biol. Chem. 279 (24) (2004) 25420–25429.
[50] C.R. Sweet, A.A. Ribeiro, C.R. Raetz, Oxidation and transamination of the 3″-position of UDP-*N*-acetylglucosamine by enzymes from *Acidithiobacillus ferrooxidans*. Role in the formation of lipid a molecules with four amide-linked acyl chains, J. Biol. Chem. 279 (24) (2004) 25400–25410.
[51] A. Yokota, M. Rodriguez, Y. Yamada, K. Imai, D. Borowiak, H. Mayer, Lipopolysaccharides of *Thiobacillus* species containing lipid A with 2,3-diamino-2,3 dideoxyglucose, Arch. Microbiol. 149 (1987) 106–111.
[52] A.C. Casabuono, C. Czibener, C.M.G. Del Giudice, E. Valguarnera, J.E. Ugalde, A.S. Couto, New features in the lipid a structure of *Brucella suis* and *Brucella abortus* lipopolysaccharide, J. Am. Soc. Mass Spectrom. 28 (12) (2017) 2716–2723.
[53] C.R. Sweet, A.A. Ribeiro, C.R.H. Raetz, Oxidation and transamination of the 3″-position of UDP-*N*-acetylglucosamine by enzymes from *Acidithiobacillus ferrooxidans* role in the formation of lipid a molecules with four amide-linked acyl chains, J. Biol. Chem. 279 (2004) 25400–25410.
[54] E.T. Rietschel, T. Krikae, F.U. Schade, U. Mamat, G. Schmidt, H. Loppnow, A.J. Ulmer, U. Zahringer, U. Seydel, F. Di Padova, M. Schreier, H. Brade, Bacterial endotoxin: molecular relationships of structure to activity and function, FASEB J. 8 (1994) 217–225.